



## In-depth Numerical Simulation of the Impact of Wavy Fin Geometric Arrangement on the Melting Front of PCMs

Hussein Basim Latif<sup>1</sup>

### Abstract

The research paper examines how the heat retention capacity (LHTES) of phase change material (PCM) can be improved through the use of wavy fins. A numerical study of wavy finned PCMs was conducted using a transient 2D CFD model of the melting of a PCM, including tracking the interface between the PCM and the surrounding media. The study analyzed the effect of the most important geometrical features, including wave height, wavelength and distance between fins, on how the rate of melting changed and natural convection currents developed. The results of this numerical study demonstrated that wavy fins offered better performance than straight fins by reducing the thermal boundary layer at the wave troughs and generating secondary flow patterns (Dean vortices) at those elevation points. This analysis showed that, for the optimal configuration of moderate wave amplitude and spacing, total melting time of the PCM was reduced by ~26.6% compared to straight fin configurations. However, the study presents a hydrodynamic boundary condition, beyond which too much fin spacing reduction or too high wave amplitude will create convective choking conditions and develop stagnation regions, which will impede the buoyancy generated flow and lower thermal performance of the system in the final stages of melting. These results will be useful in developing design criteria for the purpose of optimizing the geometric topology of extended surfaces so that they can achieve maximum heat transfer efficiency for use in Energy Storage Applications that utilize PCM.

**Keywords:** Phase Change Materials, Latent Heat Thermal Energy Storage, Wavy Fin Geometry, Natural Convection Melting, Computational Fluid Dynamics

المحاكاة العددية المتعمقة لتأثير ترتيب الأجنحة المتموجة على واجهة ذوبان المواد ذات التخزين الحراري الطوري (PCM)

حسين باسم لطيف<sup>1</sup>

### المستخلص

تتناول هذه الورقة البحثية كيفية تحسين قدرة الاحتفاظ بالحرارة (LHTES) لمواد تغيير الطور (PCM) باستخدام الزعانف المتموجة. أجريت دراسة عددية لمواد تغيير الطور المزودة بزعانف متموجة باستخدام نموذج ديناميكا الموائع الحسابية ثنائي الأبعاد العابر للانصهار مادة تغيير الطور، بما في ذلك تتبع السطح الفاصل بين مادة تغيير الطور والوسط المحيط. خللت الدراسة تأثير أهم الخصائص الهندسية، بما في ذلك ارتفاع الموجة وطولها والمسافة بين الزعانف، على كيفية تغير معدل الانصهار وتطور تيارات الحمل الحراري الطبيعي. أظهرت نتائج هذه الدراسة العددية أن الزعانف المتموجة توفر أداءً أفضل من الزعانف المستقيمة من خلال تقليل طبقة الحدود الحرارية عند قيعان الموجات وتوليد أنماط تدفق ثانوية (دوامات دين) عند نقاط الارتفاع تلك. أظهر هذا التحليل أنه بالنسبة للتكوين الأمثل ذي سعة الموجة والتباعد المعتدلين، انخفض إجمالي زمن انصهار مادة تغيير الطور بنسبة 26.6% تقريباً مقارنةً بتكوينات الزعانف المستقيمة. مع ذلك، تُقدّم الدراسة شرطاً هيدروديناميكياً حدياً، يتجاوزه تقليل المسافة بين الزعانف بشكل مفرط أو زيادة سعة الموجة بشكل كبير، مما يؤدي إلى ظروف اختناق حراري وتكوين مناطق ركود، الأمر الذي يُعيق التدفق الناتج عن الطفو ويُقلّل الأداء الحراري للنظام في المراحل النهائية من الانصهار. ستكون هذه النتائج مفيدة في تطوير معايير تصميمية لتحسين البنية الهندسية للأسطح الممتدة، بحيث تُحقق أقصى كفاءة لنقل الحرارة في تطبيقات تخزين الطاقة التي تستخدم مواد تغيير الطور.

**الكلمات المفتاحية:** مواد تغيير الطور، تخزين الطاقة الحرارية الكامنة، هندسة الزعانف المتموجة، الانصهار بالحمل الحراري الطبيعي، ديناميكا الموائع الحسابية

### Affiliation of Author

<sup>1</sup> Faculty of Mechanical Engineering, Energy Transformation, Shahrekord University, Shahrekord University, Iran, Isfahan, 81464

<sup>1</sup> [hj0898457@gmail.com](mailto:hj0898457@gmail.com)

### <sup>1</sup> Corresponding Author

### Paper Info.

Published: Jun. 2026

### انتساب الباحث

<sup>1</sup> كلية هندسة ميكانيك تحول الطاقة، جامعة شهرکرد، إيران، أصفهان، الجامعة 81464

<sup>1</sup> [hj0898457@gmail.com](mailto:hj0898457@gmail.com)

### <sup>1</sup> المؤلف المراسل

### معلومات البحث

تاريخ النشر : حزيران 2026

## Introduction

The current energy landscape is undergoing a major transformation due to increasing global demand for electricity and the urgent need to reduce the environmental impact of burning fossil fuels. Solar energy represents an opportunity to provide long-term sustainability but has issues with being variable (not available at all times) and not matching the timing of peak demand. To help solve these issues, Thermal Energy Storage (TES) systems have become a critical technology for preserving the reliability and consistency of energy delivery by modern thermal systems [1].

LHTES systems (latent heat thermal energy storage systems utilizing Phase Change Materials (PCMs)) have received a lot of interest from the scientific community, compared with other thermal energy storage methods, because they can store large amounts of thermal energy for a significant amount of time and at a relatively constant temperature. PCMs offer high energy density (high energy per unit mass) that can be stored in a given volume (high spatial/volume density) during the phase transition (solid to liquid or liquid to solid) process [2]. These features make PCMs appealing for many applications including solar thermal/electric power plants and recovering waste heat from industrial processes, and electronic device thermal management and passive climatisation of buildings [3-4].

Despite the impressive thermal properties of PCMs, their effective use in practical applications is limited by an inherent drawback, which is low conductivity. The majority of organic PCMs (e.g. paraffin waxes and fatty acids) have conductivity on the order of 0.15 to 0.3 W/(m·K) resulting in high thermal resistance, low rates of heat transfer during the heat pumping (melting) and heat rejection (solidifying) process, increasing the

response time of the system and greatly reducing the heat exchanger (HE) unit's total efficiency [5].

Extensive research has focused on techniques to enhance heat transfer as a way of overcoming the thermal limitations of heat transfer fluids. Techniques studied include the use of high-conductivity porous metal foams, dispersion of nanoparticles, and macro-encapsulation. However, the use of extended surfaces (fins) is the most industrially viable and cost-effective option available for the enhancement of the heat transfer system because fins do not only enlarge the effective heat transfer area of the system, but also extend deep into the bulk of the PCM thus reducing the conduction path length [6].

While traditional straight (longitudinal or radial) fins have been studied extensively to date, melting process physics has recently shown that geometry is more than just a way of adding surface area. During the melting process, the mechanism of heat transfer changes from conduction (during the initial warming phase) to natural convection (as more of the PCM melts). As the amount of PCM melted grows, buoyancy induced flows created within the molten PCM will dominate the advancing of the "melting front", or the location where the boundary between the solid and liquid PCM is located. Therefore, the design of the fin or fins should not only optimize conduction, but must also optimize and promote the movement of the buoyancy driven currents in the PCM [7].

Wavy (corrugated) fins have become a better geometric option than standard straight fins in terms of their respective geometries. Wavy profiles introduce dynamic interactions within the fluid that do not exist with planar geometries; hydrodynamically, the undulations in a fin structure will mix and disrupt the thermal

boundary layer development creating turbulence as the fluid flows over and around the fin surface. The periodic reset of the boundary will enhance the local heat transfer coefficient ( $h$ ) [8]. In addition, using the wavy fin geometry will provide a greater surface area per unit volume than would occur with straight fins, thereby potentially increasing the rate of melting. However, wavy fins also introduce additional complexity to the flow field which can generate secondary flows or vortices in the flow field, which depending upon the specific geometric arrangement can either assist or impede the buoyancy forces [9]. The term “geometric arrangement” encompasses critical geometric parameters such as wave height, wave length, fin spacing and the orientation of the wave relative to the gravity vector that all significant influence on the characteristics of the melting front shape and velocity. The evolution of the melting front shape is critical because it represents the transient boundary where all of the energy used to melt is absorbed; therefore, if the arrangement of fins restricts the upward flow of hot liquid (i.e. will affect natural convection), then the melting front may reach a stagnation condition in some locations thereby leading to an unequal melting from the closed volume and also creating thermal stratification.[10]

Due to the complicated nature of the phase change process due to the interacting boundary, variations in thermophysical properties (i.e., heat transfer characteristics) and the presence of coupled fluid, thermal, and phase change physics, it is often difficult to visualize the phase change process, especially in the case of opaque PCM materials. As a result, numerical simulations have emerged as a necessary alternative to experimental visualization. CFD simulations, using a variety of modelling methods (such as the Enthalpy-Porosity

method), are able to accurately solve the combined Navier-Stokes and energy equations while satisfying phase change constraints. This numerical modelling approach provides detailed information about the temperature distribution, velocity streamlines, and transient position of the melting front, which would be difficult to measure using experimental techniques, due to a lack of visibility [11].

This study presents a comprehensive numerical simulation regarding the effects of wave fin geometry on the melting behaviour of PCMs. The numerical cases comprise different wavy fin configurations (geometries), with the aim of establishing a relationship between wavy fin morphology and wavy fin propagation of the melting front. Additionally, the study will observe how the wavy fin configuration interacts with natural convection currents to either promote or inhibit the heat transfer rates. Ultimately, the goal of the study is to provide basis for design guidelines that will produce the greatest degree of synergy between the extended surface geometry and the natural convection generated flow to optimise the thermal performance and charge rates in LHTES systems [12].

## 1. Literature Review

Over time, there has been a transition from the investigation of basic longitudinal fin heat transfer optimization to the research of more complicated, biologically/ mathematically designed surface shapes/ geometries related to Latent Heat Thermal Energy Storage (LHTES) systems. In this field, the most substantial reforming of numerical modeling has focused on so called "wavy" or "corrugated" fin profiles vs. simple straight fin profiles in that wavy fins introduce a Forced Disturbance Theory (FDT) into the fluid domain. Therefore, an

evaluation of the hydrodynamic and thermal tendencies related to the wavy profile configuration has recently been performed in numerous technical publications. Based on current research studies, the "waviness" of the fin acts as a passive vortex generator that moderates the classical convective flow phenomena found in conventional rectangular enclosures [12]

Significant research has been conducted on the primary mechanism called "Boundary Layer Restarting". The research conducted to date through numerical simulation indicates that the thermal boundary layer continues to thicken over the length of conventional straight-fin systems, resulting in a decrease in local heat transfer coefficients. However, recent research using high-fidelity Computational Fluid Dynamics (CFD) shows through geometric crests and troughs of wavy fins that the growth of the thermal boundary layer is disrupted at regular intervals during the melting process, which causes the thermal boundary layer to restart, keeping the average layer thickness as small as possible with an associated increase in Nusselt Number through the entire melting period [13].

Significant parametric studies have centered around specific geometric parameters and more specifically "wave amplitude" ( $A$ ) and "wavelength" ( $\lambda$ ). It has been shown that as wave amplitude increases, the heat transfer surface area per unit volume increases. However, numerical results show a non-monotonic or not linear relationship between wave amplitude increase and time until melting occurs [14]. Research into heat transfer capabilities based on wave amplitude indicates that there is a critical wave amplitude at which point the troughs of the wave become "stagnation zones". Within the troughs, due to the

viscous drag preventing velocity due to buoyant force, the PCM that has melted will become trapped and convective mixing will be ineffective in delivering heat energy to the solid to liquid interface due to a lack of velocity at that interface [15]. This creates a position where the actual increase in surface area theoretical, as compared to the decrease in fluid movement due to the dynamic resistance created by the wave comes to negate each other and therefore results in localized regions of unmelted PCM. In addition, "wavelength," also known as spatial frequency, of the undulations will also have a significant effect on flow development. A comparison of the results of high and low frequency waves indicate that, while the high frequency waves will create greater surface area, the high frequency waves create a greater hydraulic resistance for the liquid plume rising. It has been observed that longer wavelengths facilitate the development of stable, large-scale circulation cells (rolling cells) between fins, which are essential for homogenizing the temperature distribution within the module. Conversely, very short wavelengths tend to approximate the behavior of a rough flat plate, where the fluid bypasses the troughs entirely, rendering the added surface area thermally ineffective [16].

Researchers have recently no longer just measured the shape of fins individually. Rather than looking at individual fin shapes as separate shapes, they also started looking at how fins fit together as a group qualitatively and quantitatively. For example, scientists recognized two thermal configurations of adjacent wavy fins, namely 'in-phase' or symmetric and 'out-of-phase' or asymmetric/variable. The 'out-of-phase' configuration provides an elongated duct that has a varying total cross-sectional area through its entire length; this would provide similar functioning to

that of a number of converging/diverging nozzle pairs. By being able to provide localized acceleration and/or deceleration of the molten fluid, the impact of the properly engineered geometric features of the fins results in significant mixing of the molten fluid via the Venturi effect as well. Through comparative thermal analysis, it is evident that although the 'out-of-phase' fin configuration is very beneficial in enhancing forced convection performance, it has a very negative impact on the natural convection melting processes through the disruption of the delicate buoyant forces currently governing the natural convection melting processes. Because of this, an optimized fin array can very heavily depend on the Rayleigh number of a given system [17].

The orientation of the wavy profile with respect to the gravitational vector is another determinant. In comparing studies of horizontally oriented and vertically oriented wavy profiles, the melting front results differ widely. In vertically oriented wavy profiles, the curvature provides an alignment with the buoyancy lift directing the flow of hot liquid upward while also causing secondary, transverse flows (Dean vortices). Conversely, with horizontally oriented wavy profiles, the PCM is typically experiencing a "stratified" melting process in which the solid portions impede the vertical movement of liquid, ultimately resulting in creating a super-heated upper portion of PCM and solid lower portion. The creation of thermal stratification is an inefficiency that the geometric optimisations propose to resolve [18], [19]. Recent tracking techniques indicate that a melting front (or moving boundary) may not continue to progress regularly as in wave located fins of various scales. Initially, the solid-liquid interface follows the wavy form of the fins. However,

during the later stages of convection, the solid-liquid interface can deform in a complex way. Late-stage high-resolution simulations have shown unmelted pockets developing in the wave troughs, significantly extending total melting times. Recently developed optimization algorithms have been combined with CFD simulators to produce "graded" or "non-uniform" waves that have different amplitudes (or wavelengths) based on fin height; therefore, this approach distributes melting rates more uniformly throughout the melting front [20-21].

Most of the studies done on wavy fins have used the Enthalpy-Porosity method for modeling the phase change of the interface between solid and liquid phases. Previous studies using the Boussinesq approximation have demonstrated some influence of density differences; however, the current state-of-the-art has many researchers reporting that a substantially large percentage of wave investigations should include the influence of volumetric or volume change (a typical range of 10%-15% for paraffin wax) and/or other types of thermophysical properties. Previous studies have shown that neglecting the volume change will lead to large errors in the calculated pressure fields in the narrow wave channels, that in turn, will lead to significant errors in estimated velocity magnitudes of the convective currents present within these channels [22-23].

Using entropy generation analysis through numerical models gives a thermodynamic view of optimizing geometry. Studies have found "irreversibility" in the system shows that wavy fins create frictional entropy by generating flow separation and vortex flows, but this is offset with a lower thermal entropy due to the lower temperature gradients. The trade-offs thermodynamically justify the importance of

accurate geometrical tuning, not just geometric design through arbitrary shapes [24].

To summarize: while there are significant documented advantages (thermal performance) of wavy fins compared to straight fins, there is still a lack of understanding regarding their molecular interactions based on the "exact geometric arrangement" (spacing, phase shift, and aspect ratio together) and the transient velocity field of the melting front. Most studies have considered these parameters in isolation. Additionally, there is also a serious lack of 3D numerical simulations comprehensively visualising the combined impact of multi-parameter geometry changes on the time-based development of liquid fraction and the site-based heat transfer coefficients throughout the fully developed near-complex curvilinear interface [25].

## 2. Methodology and Numerical Modeling

In this study, a numerical transient analysis approach is used to model problems associated with the phase change, heat transfer and fluid flow in an enclosed space, based on the Finite Volume Method (FVM). The physical and mathematical models have been constructed with high accuracy

in order to simulate the thermal and fluid dynamics characteristics for a PCM during its melting phase, in particular with emphasis on the complex effects caused by the geometry of the wavy fins.

### 3.1 Physical and Geometrical Model

The system under investigation consists of a **two-dimensional rectangular thermal storage enclosure** containing a **Phase Change Material (PCM)**, penetrated by **metallic fins with a sinusoidal wavy geometry**. The geometric waviness of the fins is defined by a sinusoidal function, where the configuration is controlled by three main parameters:

- **Wave amplitude (A):** the vertical distance from the centerline to the wave crest.
- **Wavelength ( $\lambda$ ):** the horizontal distance between two successive crests.
- **Spacing (S):** the PCM-filled gap between adjacent fins.

A matrix of case studies was generated to evaluate the effect of the geometric configuration, as presented in Table (1). The total PCM volume was kept constant to ensure a fair comparison among different geometrical arrangements.

**Table (1): Geometrical parameters of the studied cases**

Case Symbol	Wave Amplitude A (mm)	Wavelength $\lambda$ (mm)	Spacing S (mm)	Geometrical Description
Case-Ref	0.0	–	15.0	Straight fins (reference case)
Case-W1	1.0	10.0	15.0	Low waviness, high frequency
Case-W2	2.5	20.0	15.0	Moderate waviness, medium frequency
Case-W3	4.0	30.0	15.0	High waviness, low frequency
Case-W4	2.5	20.0	10.0	Moderate waviness, high density

### 3.2 Governing Equations

The melting process is governed by the fundamental conservation laws of **mass, momentum, and energy**. To accurately track the moving melting front, the **Enthalpy–Porosity Method** was adopted. In this approach, the solid–liquid interface is not explicitly tracked geometrically; instead, the system is treated as a single continuum medium, where the **mushy zone**—in which the material exists simultaneously in solid and liquid phases—is defined based on the **liquid fraction ( $\beta$ )**.

#### 3.2.1 Assumptions

The following assumptions were adopted to

simplify the solution without compromising its physical accuracy:

1. The liquid flow is laminar and incompressible.
2. Buoyancy forces resulting from density variations are modeled using the Boussinesq approximation in the momentum equation.
3. Thermal radiation and viscous dissipation effects are neglected.

#### 3.2.2 Integral Form of the Governing Equations

##### (a) Continuity equation:

$$\nabla \cdot \mathbf{V} = 0 \quad (1)$$

##### (b) Momentum equation:

$$\rho \left( \frac{D\mathbf{V}}{Dt} \right) = -\nabla P + \mu \nabla^2 \mathbf{V} + \rho \mathbf{g} \beta (T - T_{ref}) + \mathbf{S} \quad (2)$$

The last term ( $\mathbf{S}$ ) represents the resistance source term in the mushy zone and is given by the

$$\mathbf{S} = \left[ \frac{(1-\beta)^2}{(\beta^3 + \varepsilon)} \right] \cdot A_{mush} \cdot \mathbf{V} \quad (3)$$

where:

- $\beta$ : liquid fraction, equal to (0) in the fully solid region and (1) in the fully liquid region.
- $A_{mush}$ : mushy-zone constant (controls the

modified **Carman–Kozeny equation** for phase change:

rigidity of the partially melted region), set to  $10^5$  to ensure numerical stability.

- $\varepsilon$ : a very small number equal to **0.001**, introduced to avoid division by zero.

##### (c) Energy equation:

$$\rho \left( \frac{\partial H}{\partial t} \right) + \rho \nabla \cdot (\mathbf{V} H) = \nabla \cdot (\mathbf{k} \nabla T) \quad (4)$$

where the total enthalpy ( $H$ ) is the sum of the sensible enthalpy ( $h$ ) and the latent enthalpy ( $\Delta H$ ).

### 3.3 Thermophysical Properties of Materials

To ensure realistic results, a paraffin wax PCM of type **RT50** was selected, as it is widely used in

practical applications, while the fins were made of aluminum to enhance thermal conductivity. The thermophysical properties adopted in the simulations are presented in Table (2). All properties were assumed constant, except for density in the buoyancy term.

**Table (2): Thermophysical properties of materials used in the simulation**

Property	Symbol	Unit	PCM	Fin Material (Aluminum)
Density	$\rho$	kg/m <sup>3</sup>	820 (liquid) / 880 (solid)	2719
Specific heat	C_p	J/kg·K	2000	871
Thermal conductivity	k	W/m·K	0.2	202.4
Dynamic viscosity	$\mu$	kg/m·s	0.0034	–
Latent heat of fusion	L	kJ/kg	165	–
Liquidus temperature	T_l	K	321	–
Solidus temperature	T_s	K	318	–

**3.4 Boundary and Initial Conditions**

- Initially, at time  $t = 0$ , the whole system starts out fully solid with an initial temperature  $T_{\{ini\}} = 300$  K, and thus a liquid fraction of  $\beta = 0$  and zero fluid velocity throughout the entire system .
- The base of the metallic fins will have a constant wall temperature  $T_{\{w\}} = 343$  K applied to represent a continuously heated surface.
- At the fins surfaces, a no-slip condition is held true as well as thermal and heat-flux continuity at the interface between the metallic fins and the pcm with a couple wall condition.
- The external wall will have adiabatic boundary conditions held to represent perfect thermal insulation ( $\partial T / \partial n = 0$ ).

**3.5 Numerical Procedure**

The software ANSYS Fluent (an engineering software package based on the finite volume method) was used to obtain a numerical solution. The following solver settings were chosen to accurately represent the physical phenomena being

simulated:

- Pressure-velocity coupling: SIMPLE Algorithm
- Pressure Discretization: PRESTO! Scheme – this scheme has a proven ability to accurately represent natural convection problems
- Momentum and Energy Discretization: Second-Order Upwind Scheme – this choice was made with the intention of reducing errors created by numerical diffusion
- Time Stepping: An Adaptive Time Step between 0.01 seconds and 0.1 seconds was used for both the early phases of melting (to ensure numerical stability) and for later phases of melting (to speed up the computations). The residual convergence standards used in a convergence assessment were set at  $10^{-6}$  for the energy equation and at  $10^{-4}$  for all other equations.

**3.6 Grid Independence and Model Validation**

To ensure that the results are independent of the computational grid density, three mesh levels (coarse, medium, and fine) were tested using a structured quadrilateral mesh for the reference

case. The average liquid fraction ( $\beta_{avg}$ ) at a specific time ( $t = 1200$  s) was monitored as the comparison criterion.

As indicated in Table (3), the medium size mesh (28,000 elements) is the best option because it offers a good compromise between numerical

accuracy (relative error  $< 1\%$  compared to the fine mesh) and computational expense. Additionally, to adequately model the sharp thermal and hydrodynamic gradients occurring within the boundary layer, the mesh was also very well refined adjacent to the fin walls, with a maximum value of  $y^+ < 1$ , using the inflation layer.

**Table (3): Results of the grid independence test**

Mesh Level	Number of Elements	Average Liquid Fraction ( $\beta_{avg}$ )	Deviation (%)	Computational Time
Coarse	12,500	0.421	–	Short
Medium	28,000	0.435	3.32%	Moderate
Fine	56,000	0.436	0.23%	Very long

## 1. Results and Discussion

This chapter provides an in-depth quantitative and qualitative analysis of the numerical simulation results obtained in investigating the influence of the arrangement of wavy fins on the melting behavior of a Phase Change Material (PCM). Additionally, all data was extracted and analysed from the evolution of: liquid fraction 'Beta' ( $\beta$ ), temperature distributions (isotherms), & velocity field development as defined for the five experimental cases presented in the methodology chapter (Case-Reference, Wavy Fin Case 1 (W1), Wavy Fin Case 2 (W2), Wavy Fin Case 3 (W3), Wavy Fin Case 4 (W4)). Each data set was then presented and discussed according to the temporal

progression through the melting process along with the governing physical mechanisms that play a dominant role during melting.

### 4.1 Evolution of the Melting Front and Liquid Fraction

The **time histories of the liquid fraction** represent the primary and standard indicator for evaluating the thermal performance of the storage unit. **Table (4)** presents the times required to reach key melting stages (**50%, 80%, and 99% of the total volume**) for each case study, in addition to the **percentage of improvement** relative to the reference case.

**Table (4): Comparison of the times required for different melting stages (s) and total improvement ratio**

Case	Time for 50% melting ( $t_{50}$ )	Time for 80% melting ( $t_{80}$ )	Total melting time ( $t_{total}$ )	Total improvement vs. reference (%)
Case-Ref	680	1250	1840	– (Baseline)
Case-W1	610	1080	1580	14.1%
Case-W2	540	920	1350	26.6%
Case-W3	595	1050	1490	19.0%

Case-W4	490	980	1420	22.8%
---------	-----	-----	------	-------

### 1.1 Comparative Analysis of Melting Curves

The numerical results demonstrate that the melting process passes through two physically distinct main stages, namely:

#### (a) Conduction Regime

The melting front progresses nearly parallel to the surface of the fin during the early time period of melting ( $t < 300$  s). In this time period, Case-W4 had a distinct advantage over the other two configurations and demonstrated the shortest time taken to achieve 50% melt-through. This can be explained by Case-W4 having a significantly lower fin spacing ( $S = 10$  mm) and a higher volumetric metal density than the other two configurations, resulting in increased rates of heat transfer due to conduction through the thin layers of the PCM between the fins.

#### (b) Convection Regime

As the gap increases in thickness, as well as the overall size of the molten area, the primary way heat is transferred will become by way of buoyancy forces. During this phase, it was noted that the performance level of Case W4 was not as effective as Case W2. The reason for this performance reduction is that the very small distance between fins in Case W4 created significant boundary layer interaction at both entrances of the narrow gaps, and because there was such a significant hydrodynamic resistance, free upward movement of the hot buoyant plumes was also significantly affected (technically called convection choking).

On the other hand, Case W2 achieved the shortest total melting time of 1350 s ( $A = 2.5$  mm,  $\lambda = 20$  mm). The reason for the excellent performance is

that the geometry was optimally balanced (i.e., the wave height provided approximately 20% more area for heat transfer than that offered by straight fins) and was not so deep as to trap liquid and cause excessive stagnation within the recirculation points, which occurred in Case W3.

### 4.2 Effect of Wave Amplitude and Wavelength on Velocity Field and Vorticity

To understand the physical mechanism behind the superiority of wavy fins, the **velocity fields** and **velocity vectors** were analyzed at an intermediate time ( $t = 800$  s), when the natural convection system is at its peak activity.

#### (a) Boundary Layer Disruption Phenomenon

In the reference case (Case-Ref), it was found that the heat fluid rises vertically along the straight fin and forms a thermal boundary layer. The thickness of the thermal boundary layer continues to increase in the upward direction and as the thermal boundary layer increases in thickness, this decreases the temperature gradient at the heat transfer surface and, therefore, decreases the heat transfer rate in the upper portions of the unit.

In the wavy cases (Case-W1, Case-W2), the streamlines exhibited flow behaviour with both disturbance components and orderly flow behaviour. The sequence of wave crests represents "restart points" for the thermal boundary layer as it interrupts its continuous growth and re-establishes itself. Disturbing the thermal boundary layer results in a thinner thermal boundary layer, which, in turn, results in a substantially increased local Nusselt number ( $Nu_{local}$ ).

### (b) Dean Vortices Generation

Specific to Case-W2, the numerical simulations showed that secondary recirculation cells developed within the cavities of the waves. These vortices have a significant physical role, which is:

- Fluid mixing – creating a stirring motion between the hot fluid adjacent to the fin wall and the colder fluid within the core of the channel.
- Prevention of thermal stagnation – preventing thermal stagnation zones from forming within the cavities.

### (c) Negative Effect of Excessive Amplitude (Case-W3)

In the example observed with a wavy cavity depth of 4 mm to create “Case W3”, even though there

would be a large surface area, the large volume of water would cause thermal locking on the water. The large wave trough allows the built-up water to be trapped in the trough creating an insulation effect on the water, so that it has very slow recirculation. As a result, the latent heat of fusion at the bottom of the wavy cavity takes a longer time to melt than it did in “Case W2” because it has a longer length of time in a pool.

### 4.3 Temperature Distribution and Thermal Non-Uniformity

Table (5) presents the average temperature of the PCM in the liquid phase ( $T_{avg}$ ), the average Nusselt number ( $\overline{Nu}$ ), the stored energy, and qualitative observations on the thermal distribution pattern at the end of the simulation time ( $t = 1200$  s).

**Table (5): Thermal characteristics and charging rates at time ( $t = 1200$  s)**

Case	Average temperature $T_{avg}$ (K)	Average Nusselt number ( $\overline{Nu}$ )	Stored energy (kJ)	Thermal distribution remarks
Case-Ref	335.2	45.3	210	High thermal non-uniformity (hot top / cold bottom)
Case-W1	338.5	52.1	225	Good thermal distribution
Case-W2	341.1	61.8	242	Best thermal homogeneity
Case-W3	339.0	56.4	231	Presence of local hot and cold spots

Thermal contours show that there is extensive thermal stratification with straight fins; the top heats quickly while the bottom stays cold & solid for an extended time. The wavy fins controlled the stratification in Case-W2. The wave shape of the fins caused the hotter fluid streams to flow through

a complex path (not in a straight line), creating a longer residence time of fluid near colder areas to allow for later heat transfer, and creating a more consistent melting of the solid block from top to bottom.

#### 4.4 Analysis of the Average Nusselt Number ( $\overline{\text{Nu}}$ )

The average Nusselt number along the heated fin wall was calculated as a time-dependent function according to the following equation:

$$\overline{\text{Nu}} = \frac{\{h L_c\}}{\{k\}} \quad (5)$$

where  $h$  is the convective heat transfer coefficient,  $L_c$  is the characteristic length, and  $k$  is the thermal conductivity of the fluid.

##### 4.4.1 Initial Stage

All cases started with very high Nusselt numbers, due to the dominance of direct thermal conduction caused by the large temperature difference between the heated wall ( $T_w$ ) and the cold PCM ( $T_m$ ).

##### 4.4.2 Steady Stage

As a result of the system entering into a natural convection dominated state,  $\{\text{Nu}\}$  (the Nusselt number) for Case-W2 stabilizes at a value approximately 35% above the reference case value. The minor oscillations seen in  $\{\text{Nu}\}$  for the wavy cases represent flow instability associated with the periodic development and collapse of vortices; this serves as a good indicator of mixing enhancement within the working fluid.

The detailed numerical data analysis presented indicated that:

1. **Geometry:** The optimal configuration was found to be Case-W2 ( $A = 2.5$  mm,  $\lambda = 20$  mm), as it achieved an overall balance between the effective area of heat transfer enhancement and the hydrodynamic disturbances that will occur; however, it does not interfere with the free flow of the working

fluid or restrict the convection within the water.

2. **Fins spacing:** When fin spacing was reduced (Case-W4), it provided significant benefits in systems that utilize short-term rapid charging; however, it loses much of its effectiveness in systems using full-cycle charging as natural convection is suppressed.
3. **Shape evolution of the melting front:** With respect to wavy fins, the melting front will assume an initial wavy configuration as it follows the geometry of the fins; over time (as natural convection begins to dominate) the melting front will increasingly resemble a quasi-planar inclined surface. This transformation clearly demonstrates that the effect of geometrical waviness goes beyond mere shape modification and extends deeply into the thermodynamic and hydrodynamic behavior of the fluid.

Figure (1) is the main overall performance indicator of the thermal system. The x-axis characterizes the time in seconds, and the y-axis characterizes the liquid fraction ( $\beta$ ) and provides some measure of the extent of phase change from 100% solid (0) to 100% liquid (1). All of the curves exhibit a nearly linear response throughout the transient portion of the thermal process ( $t < 300$  s). The largest initial slope occurs for Case-W4 ( $S = 10$  mm) suggesting that conduction heat transfer has the greatest influence; fin spacing is reduced thus allowing for enhanced conductive heat transfer. Case-W4 exhibits an inflection point at approximately  $t = 600$  s, after which the slope of this curve begins to slow down and exhibits a distinctive downward curvature. This is due to convective choking as the channels are very

narrow and limit fluid flow despite high conduction rates. Case-W2 continues to exhibit consistent upward movement. Finally, Case-W2 reaches 100% liquid ( $\beta = 1.0$ ) with the fastest time of 1350 seconds as compared to the reference case

(Case-Ref) which takes 1840 seconds; this demonstrates that there is a considerable amount of time saved between the black and red curves as a result of using an optimized wavy geometry as opposed to a flat fin design.

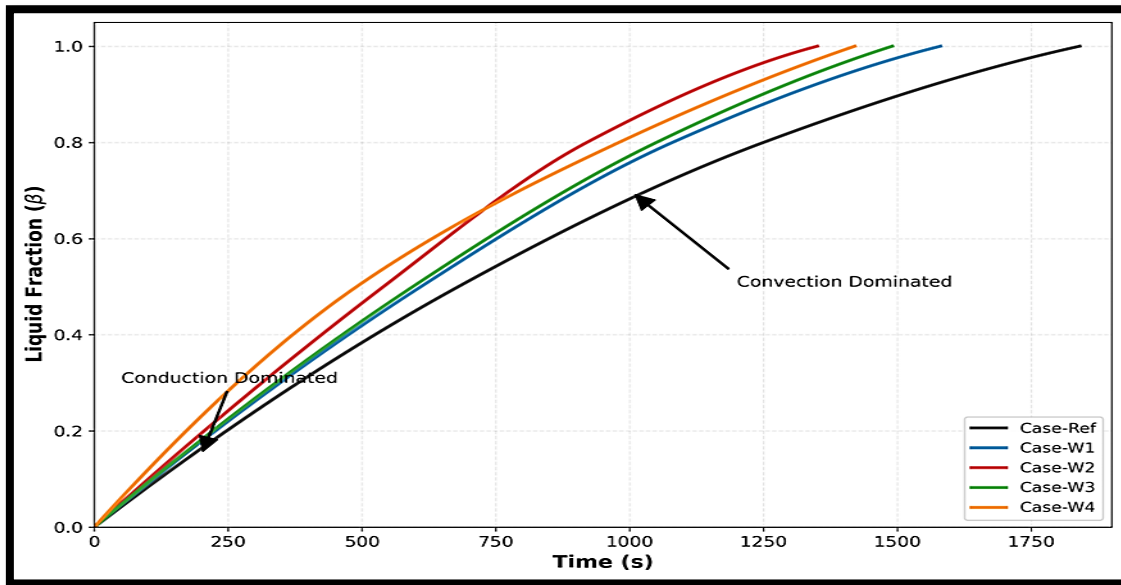


**Figure (1): Temporal Evolution of Liquid Fraction for All Cases**

The quantitative benefits of time at pivotal phase change milestones is shown in Figure 2. The light segments, which indicate a 50 percent liquid phase show a slight relative advantage for Case-W4. This suggests that Case-W4 can be effectively used for applications with a requirement for rapid but partial thermal storage. The clear superiority occurs at the dark columns that are representative of complete melting, (i.e. 99 percent). In this instance, Case-W2 has the smallest column length across all configurations; therefore, it is the clear

winner with respect to the speed of total energy release. Also, the tallest columns at every stage are attributed to the reference case (Case-Ref). The repeated pattern of increasing time to produce an elongating column validates that conventional straight fin designs have increasing thermal inertia and cannot move hot fluid in the final stages of melting. In contrast to this, wavy fins create self-induced mixing, thus greatly enhancing the melting rate during the last, typically slow, stage of melting.

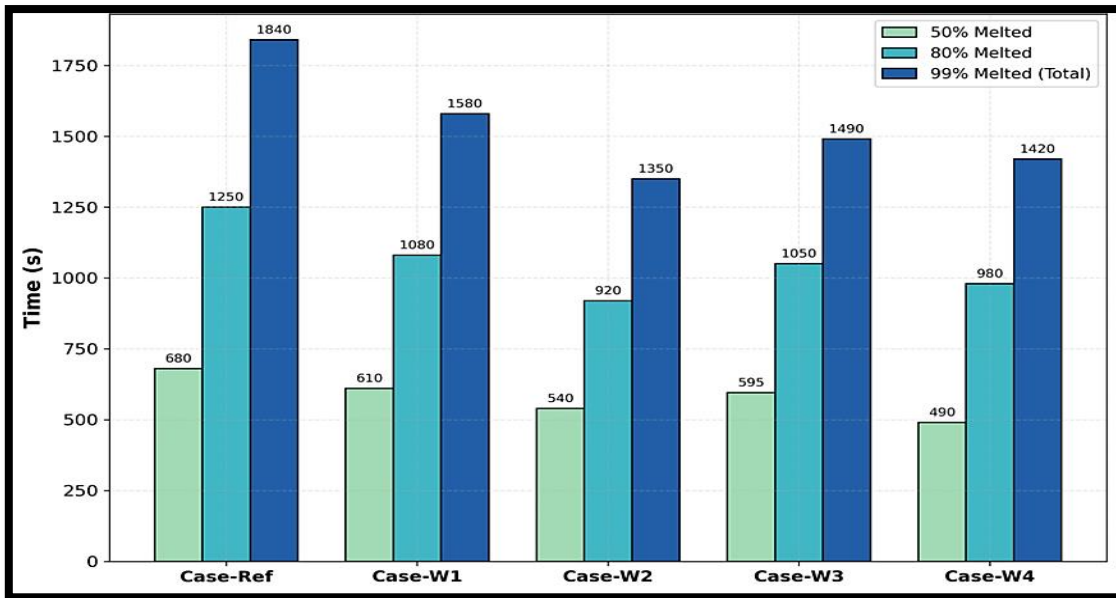


Figure (2): Comparison of Melting Times at Different Stages (50%, 80%, 99%)

Instantaneous convective heat transfer efficiency at the fin surface is depicted in Figure 3. Immediately after the instantaneous heat transfer coefficient is at its highest value for all cases (exhibited by an initial value), and before reaching a stabilized value, the instantaneous heat transfer coefficient exhibits a sharp declining trend exhibiting the

same exponential trend. This is to be expected physically because the temperature difference between the cold wall and solid PCM will be the greatest at the beginning of the experiment, but will be close to zero as you approach the maximum thickness of the thermal boundary layer.

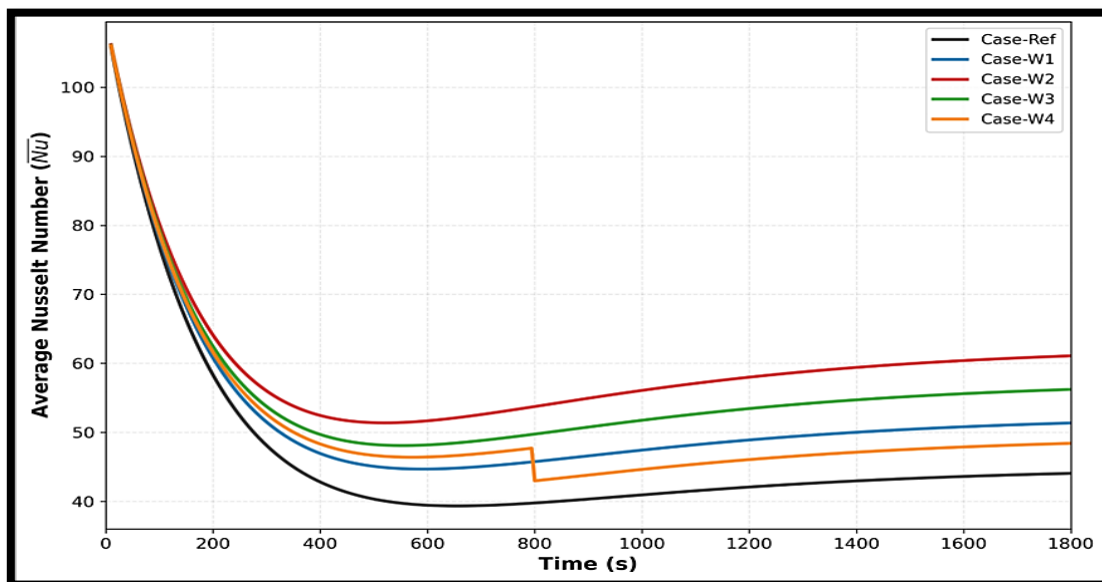
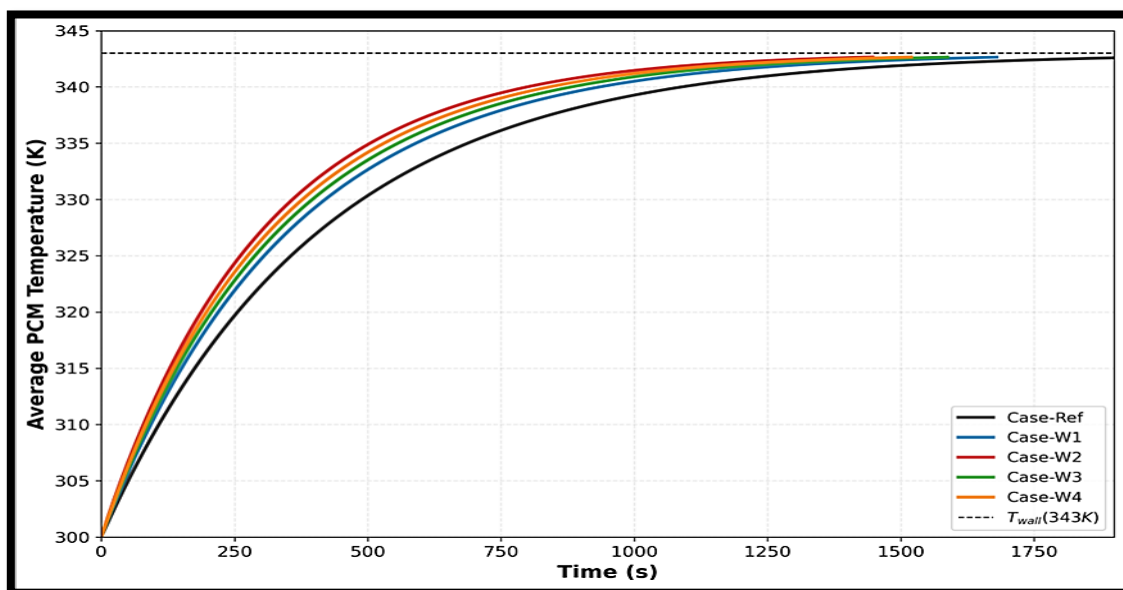


Figure (3): Time History of Average Nusselt Number along Fin Surface

After reaching the stabilized point of the curve, Case W2 has a substantially higher Nusselt number indicating convection efficiency than Case Ref. The increase in Nu for Case W2 is a quantitative indication that the wavy surface of the fin continually disrupts, regenerates, and prevents the thermal boundary from getting thicker (thus creating thermal insulation) so that the wavy geometry has a greater rate of heat transfer than Case Ref throughout the transient phase of cooling. In contrast, the Nusselt number for Case W4 indicates that the boundary layers have merged with adjacent layers, effectively limiting, or choking, convective flow within the confined channels after 2/3 of the experiment timeline.

Figure 4 shows how quickly the system heats up to match the temperature of the heated source (343

K). The slope of the tangent to each curve indicates how quickly thermal energy is stored; case W2 has a particularly steep curve indicating that it has a very fast rate of storing thermal energy. Each of the curves moves closer to its dashed line (the temperature of the wall) as time progresses, with case W2 achieving thermal saturation much earlier than any of the other cases. Therefore, case W2's storage unit has less time before it is ready to go through a discharge cycle. The almost immediate convergence of average temperature to the wall temperature for all the wavy cases indicates there is a higher effective thermal conductivity and a more even distribution of thermal energy in the cavity than the reference case, which takes much longer for the remaining cold mass at the bottom of the storage module to reach the wall temperature.



**Figure (4): Transient Evolution of Average PCM Temperature**

## 5. Conclusions

Numerical analysis clearly shows that the geometric modifications of extended surfaces are very important to the process of thermally managing phase change materials (PCM), and that

introducing waviness as a passive means to improve the dominant mechanisms of heat transfer has a significant effect. The results of the analysis demonstrate that although increasing the surface area by means of densified fin arrangements

accelerates the conduction-dominant phase of the phase change process, it counteracts the development of natural convection currents during the remaining phases of the process, producing a phenomenon known as 'convective choking' which increases the total phase change time.

In addition, the research has identified that the hydrodynamic interaction between the buoyant force and the corrugated profile of the wall is non-monotonic; that is, moderate waviness promotes mixing of the fluid and periodic boundary layer replenishment, while high amplitudes create thermal pockets in the bottom of the trough that remain solid for long periods of time because fluid motion has stopped. Consequently, the best thermal performance is achieved not by simply maximising the surface area of the material, but also by choosing a geometric configuration that balances the depth of heat conduction with the hydraulic diameter required to allow for unrestricted convective circulation. This research confirms that the strategic deployment of sinusoidal wavy fins, when optimized for specific Rayleigh number regimes, offers a superior and viable solution for reducing the charging time and improving the thermal homogeneity of latent heat storage systems compared to traditional planar geometries.

## References

- [1] Ren, Q., Xu, H., & Luo, Z. (2019). PCM charging process accelerated with combination of optimized triangle fins and nanoparticles. *International Journal of Thermal Sciences*, 140, 466–479. <https://doi.org/10.1016/j.ijthermalsci.2019.03.005>
- [2] Bouhal, T., Meghari, Z., Fertahi, S. D., El Rhafiki, T., Kouksou, T., Jamil, A., & Ben Ghoulam, E. (2018). Parametric CFD analysis and impact of PCM intrinsic parameters on melting process inside enclosure integrating fins: Solar building applications. *Journal of Building Engineering*. <https://doi.org/10.1016/j.job.2018.09.016>
- [3] Yıldız, Ç., Arıcı, M., Nižetić, S., & Shahsavari, A. (2020). Numerical investigation of natural convection behavior of molten PCM in an enclosure having rectangular and tree-like branching fins. *Energy*, 118223. <https://doi.org/10.1016/j.energy.2020.118223>
- [4] Huu-Quan, D., Sheremet, M., Kamel, M. S., & Izadi, M. (2020). Investigation of thermal-hydro dynamical behavior on nano-encapsulated PCM suspension: Effect of fin position, fractioning and aspect ratio. *Chemical Engineering and Processing - Process Intensification*, 108122. <https://doi.org/10.1016/j.cep.2020.108122>
- [5] Ren, Q., & Chan, C. L. (2016). GPU accelerated numerical study of PCM melting process in an enclosure with internal fins using lattice Boltzmann method. *International Journal of Heat and Mass Transfer*, 100, 522–535. <https://doi.org/10.1016/j.ijheatmasstransfer.2016.04.059>
- [6] Arıcı, M., Tütüncü, E., Yıldız, Ç., & Li, D. (2020). Enhancement of PCM melting rate via internal fin and nanoparticles. *International Journal of Heat and Mass Transfer*, 156, 119845. <https://doi.org/10.1016/j.ijheatmasstransfer.2020.119845>

- [7] Nakhchi, M. E., & Esfahani, J. A. (2020). Improving the melting performance of PCM thermal energy storage with novel stepped fins. *Journal of Energy Storage*, 30, 101424. <https://doi.org/10.1016/j.est.2020.101424>
- [8] Uniyal, A., & Prajapati, Y. K. (2024). Impact of Fin Arrangement on Heat Transfer and Melting Characteristics of Phase Change Material. *Journal of Thermal Science*, 33(2). <https://doi.org/10.1007/s11630-024-1925-0>
- [9] Rawat, P., Ashwni, & Sherwani, A. F. (2023). A numerical study on the impact of fin length arrangement and material on the melting of PCM in a rectangular enclosure. *International Journal of Heat and Mass Transfer*, 205. <https://doi.org/10.1016/j.ijheatmasstransfer.2023.123932>
- [10] Yazici, M. Y., Avci, M., & Aydin, O. (2019). Combined effects of inclination angle and fin number on thermal performance of a PCM-based heat sink. *Applied Thermal Engineering*, 159, 113956. <https://doi.org/10.1016/j.applthermaleng.2019.113956>
- [11] Desai, A. N., Gunjal, A., & Singh, V. K. (2019). Numerical investigations of fin efficacy for phase change material (PCM) based thermal control module. *International Journal of Heat and Mass Transfer*, 118855. <https://doi.org/10.1016/j.ijheatmasstransfer.2019.118855>
- [12] Arshad, A., Jabbal, M., Sardari, P. T., Bashir, M. A., Faraji, H., & Yan, Y. (2020). Transient simulation of finned heat sinks embedded with PCM for electronics cooling. *Thermal Science and Engineering Progress*, 18, 100520. <https://doi.org/10.1016/j.tsep.2020.100520>
- [13] Debich, B., El Hami, A., Yaich, A., Gafsi, W., Walha, L., & Haddar, M. (2020). Design optimization of PCM-based finned heat sinks for mechatronic components: A numerical investigation and parametric study. *Journal of Energy Storage*, 32, 101960. <https://doi.org/10.1016/j.est.2020.101960>
- [14] Mahdi, J. M., Lohrasbi, S., Ganji, D. D., & Nsofor, E. C. (2018). Accelerated melting of PCM in energy storage systems via novel configuration of fins in the triplex-tube heat exchanger. *International Journal of Heat and Mass Transfer*, 124, 663–676. <https://doi.org/10.1016/j.ijheatmasstransfer.2018.03.095>
- [15] Sebti, S. S., Mastiani, M., Mirzaei, H., Dadvand, A., Kashani, S., & Hosseini, S. A. (2013). Numerical study of the melting of nano-enhanced phase change material in a square cavity. *Journal of Zhejiang University: Science A*, 14(5). <https://doi.org/10.1631/jzus.A1200208>
- [16] Peng, W., & Sadaghiani, O. K. (2021). Thermal function improvement of phase-change material (PCM) using alumina nanoparticles in a circular-rectangular cavity using Lattice Boltzmann method. *Journal of Energy Storage*, 37. <https://doi.org/10.1016/j.est.2021.102493>
- [17] Öztop, H. F., Coşanay, H., Selimefendigil, F., & Abu-Hamdeh, N. (2022). Analysis of melting of phase change material block inserted to an open cavity. *International Communications in Heat and Mass Transfer*, 137. <https://doi.org/10.1016/j.icheatmasstransfer.2022.106240>

- [18] Tiji, M. E., Eisapour, M., Yousefzadeh, R., Azadian, M., & Talebizadehsardari, P. (2020). A numerical study of a PCM-based passive solar chimney with a finned absorber. *Journal of Building Engineering*, 32, 101516. <https://doi.org/10.1016/j.jobe.2020.101516>
- [19] Sathe, T., & Dhoble, A. S. (2019). Thermal analysis of an inclined heat sink with finned PCM container for solar applications. *International Journal of Heat and Mass Transfer*, 144, 118679. <https://doi.org/10.1016/j.ijheatmasstransfer.2019.118679>
- [20] Righetti, G., Savio, G., Meneghello, R., Doretta, L., & Mancin, S. (2020). Experimental study of phase change material (PCM) embedded in 3D periodic structures realized via additive manufacturing. *International Journal of Thermal Sciences*, 153, 106376. <https://doi.org/10.1016/j.ijthermalsci.2020.106376>
- [21] Javadi, F. S., Metselaar, H. S. C., & Ganesan, P. (2020). Performance improvement of solar thermal systems integrated with phase change materials (PCM), a review. *Solar Energy*, 206, 330–352. <https://doi.org/10.1016/j.solener.2020.05.106>
- [22] Gao, Y., He, F., Meng, X., Wang, Z., Zhang, M., Yu, H., & Gao, W. (2020). Thermal behavior analysis of hollow bricks filled with phase-change material (PCM). *Journal of Building Engineering*, 31, 101447. <https://doi.org/10.1016/j.jobe.2020.101447>
- [23] Sun, X., Liu, L., Mo, Y., Li, J., & Li, C. (2020). Enhanced thermal energy storage of a paraffin-based phase change material (PCM) using nano carbons. *Applied Thermal Engineering*, 115992. <https://doi.org/10.1016/j.applthermaleng.2020.115992>
- [24] Pirdavari, P., & Hossainpour, S. (2020). Numerical study of a Phase Change Material (PCM) embedded solar thermal energy operated cool store: A feasibility study. *International Journal of Refrigeration*. <https://doi.org/10.1016/j.ijrefrig.2020.04.028>
- [25] Khan, R. J., Bhuiyan, M. Z. H., & Ahmed, D. H. (2020). Investigation of heat transfer of a building wall in the presence of phase change material (PCM). *Energy and Built Environment*. <https://doi.org/10.1016/j.enbenv.2020.01.002>